Available online at www.sciencedirect.com

ScienceDirect

journal homepage: www.intl.elsevierhealth.com/journals/dema

Osseointegration: Hierarchical designing encompassing the macrometer, micrometer, and nanometer length scales

Paulo G. Coelho[a,b,c,*], *Ryo Jimbo*[d,1], *Nick Tovar*[a,2], *Estevam A. Bonfante*[e,3]

[a] *Department of Biomaterials and Biomimetics, New York University, 345 East 24th Street, Room 804s, New York, NY 10010, United States*

[b] *Director for Research, Department of Periodontology and Implant Dentistry, New York University, United States*

[c] *Affiliated Faculty, Division of Engineering, New York University Abu Dhabi, United Arab Emirates*

[d] *Department of Prosthodontics, Faculty of Odontology, Malmö University, SE 205 06 Malmö, Sweden*

[e] *Department of Prosthodontics, University of São Paulo – Bauru College of Dentistry, Al. Otávio Pinheiro Brisola 9-75, 17.012.901 Bauru, SP, Brazil*

ARTICLE INFO

Keywords:
Review
Osseointegration
Design
Macrogeometry
Surface

ABSTRACT

Objective. Osseointegration has been a proven concept in implant dentistry and orthopedics for decades. Substantial efforts for engineering implants for reduced treatment time frames have focused on micrometer and most recently on nanometer length scale alterations with negligible attention devoted to the effect of both macrometer design alterations and surgical instrumentation on osseointegration. This manuscript revisits osseointegration addressing the individual and combined role of alterations on the macrometer, micrometer, and nanometer length scales on the basis of cell culture, preclinical *in vivo* studies, and clinical evidence.

Methods. A critical appraisal of the literature was performed regarding the impact of dental implant designing on osseointegration. Results from studies with different methodological approaches and the commonly observed inconsistencies are discussed.

Results. It is a consensus that implant surface topographical and chemical alterations can hasten osseointegration. However, the tailored combination between multiple length scale design parameters that provides maximal host response is yet to be determined.

Significance. In spite of the overabundant literature on osseointegration, a proportional inconsistency in findings hitherto encountered warrants a call for appropriate multivariable study designing to ensure that adequate data collection will enable osseointegration maximization and/or optimization, which will possibly lead to the engineering of endosteal implant designs that can be immediately placed/loaded regardless of patient dependent conditions.

* *Corresponding author at*: Department of Biomaterials and Biomimetics, New York University, 345 East 24th Street, Room 804s, New York, NY 10010, United States. Tel.: +1 212 998 9214; mobile: +1 646 334 9444.

E-mail addresses: pgcoelho@nyu.edu (P.G. Coelho), ryo.jimbo@mah.se (R. Jimbo), nicktovar@gmail.com (N. Tovar), estevamab@gmail.com (E.A. Bonfante).

[1] Tel.: +46 40 665 8679; mobile: +46 70 203 1025.

[2] Tel.: +1 973 464 9556.

[3] Tel.: +55 14 3235 8272; mobile: +55 14 98153 0860.

http://dx.doi.org/10.1016/j.dental.2014.10.007

1. Introduction

Bone fusing to titanium was described in 1940 by Bothe et al [1], then by Leventhal more than 6 decades ago [2], who also showed that titanium failed to cause tissue reaction and that it would serve as an ideal metal for prostheses. After considerable time, the term osseointegration was created and it was then refined by a series of well-characterized scientific reports by Brånemark and colleagues [3,4]. It has been defined as the formation of a direct interface between an implant and bone without soft tissue interposition at the optical microscopy level [3,5]. This phenomenon has been the basis for multiple orthopedic and dental rehabilitation procedures, paving the way for quality of life improvement of a large number of patients [6].

The introduction of titanium and its alloys to implant dentistry has marked an era where the main driving force for advances in implant engineering has been centered at decreasing or eliminating the hiatus between surgical placement and functional loading due to improved host-to-implant response [7–10]. Nonetheless, clinical and basic research on the field of implant dentistry resulted in a lack of sequential and hierarchical approach for implant designing that challenges biomedical engineers to retrospectively address the interaction of the main design parameters such as macrogeometry, microgeometry, nanogeometry, and surgical instrumentation in an objective fashion [11].

The implant design is one of the important parameters for the achievement of osseointegration, however, as of today, the optimal design for atemporal implant stability in bone is yet to be determined [12–16]. Atemporal osseointegration became an academic and industrial goal since it would allow clinicians to rehabilitate patients in minimal treatment time frames [17].

This review manuscript revisits osseointegration in a structured format, first addressing how implant hardware design (bulk device design and related surgical instrumentation dimensions) features potentially influence bone healing pathway and the placement of other design parameters within implant hardware. Second, the effect of micrometer designing (a primary hardware *ad-hoc*) on osseointegration is discussed in light of the current literature. Third, and due to its more recent body of literature, a section on the available evidence and utilization of nanotechnology (a secondary *ad-hoc*) applied to implant surface engineering is presented based on their potential in further improving osseointegration when hierarchically applied onto the implant macrometer and micrometer design.

2. The effect of implant macrogeometric (hardware design) in bone healing pathway: implications for micrometer scale designing

It has been extensively reported that as time elapses following implantation of osteoconductive endosteal implants (*e.g.* titanium-based alloys), intimate contact between bone and device will render the system biomechanical stability and load-bearing capability [18–21]. Such observation has been supported by over ten thousand scientific reports that are based on a large number of different devices surgically placed in bone through a large variation in surgical instrumentation technique and sequence. Thus, even though through the course of over seven decades, osseointegration has gone from novelty to commodity in surgery, substantial attention is still devoted in understanding its principles and characteristics especially as a function of endosteal implant modification. While a plethora of studies concerns the effects of micrometer and more recently nanometer scale design parameter contribution to osseointegration, a significantly smaller body of work is available regarding how hardware design aspects affect osseointegration. For instance, far less explored in the literature is how osseointegration temporally occurs around endosteal implants substantially shift as a function of two major key implant design parameters: implant macrogeometry and its associated surgical instrumentation [22–24]. While it is obvious that two different design parameters are under consideration, their contribution to the healing mode cannot be considered separately [22,23].

2.1. *The interfacial remodeling (tight fit) healing pathway*

The healing scenario described in this section is typically observed for tight fit screw type implants (*i.e.* the majority of implant systems available in the market) as they are placed in the osteotomy in intimate contact between the implant and bone throughout the device's threaded bulk. Such intimate interplay between device and osteotomy dimensions renders the system initial or primary stability where no biologic interplay yet exists [25,26]. This mechanical interlocking is variably influenced by the implant geometry and surface micrometer level topography, as well as the implant osteotomy site dimensions, and regulate the distribution of strain applied to the hard tissue in proximity with the implant [21,27,28]. Strain is directly related to bone-implant interfacial stress and frictional force, and is clinically expressed as insertion torque [20,25,29].

The theoretical background of the primary stability concept is that the bone is assumed to be an elastic material and that strain and implant stability will have a linear relation [25]. However, in reality, the stability of the implant would decrease beyond the yield strain of the bone due to excessive microcrack formation and compression necrosis, which both phenomena trigger bone remodeling [25,30,31]. Thus, high degrees of insertion torque must be questioned since elastic theory predicts that excessive strain not only leads to the decrease of biomechanical stability, but also incites negative biologic responses depending on the implant thread design that influence the compression [17]. Such cell-mediated bone resorption and subsequent bone apposition most often occurring from the pristine bone wall toward the implant surface is responsible for what has under theoretical [32] and experimental [33] basis been coined as implant stability dip, where primary stability obtained through the mismatch between implant macrogeometry and surgical instrumentation dimensions is lost due to the cell-mediated interfacial remodeling to be regained through bone apposition [32,34].

This healing mode sequence concerns implant placement in sites that were surgically instrumented to dimensions

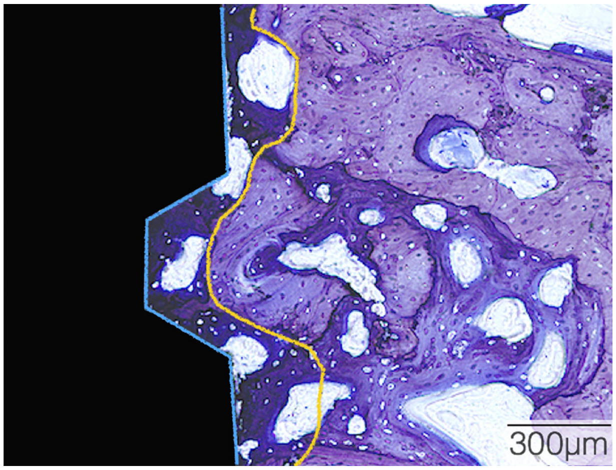

Fig. 1 – Representative optical micrograph of a screw type implant placed in a rabbit tibia instrumented to the inner diameter of the implant thread. The blue line depicts the implant perimeter that was in direct contact with bone immediately after placement (the cortical plate fully occupied the region between the blue and yellow lines). The yellow line depicts the distance from the implant surface (blue line) which cell mediated interfacial remodeling occurred due to osteocompression and/or bone cracking. The dark stained bone tissue between the blue and yellow lines is bone formed after a void space is created due to interfacial remodeling to eliminate tissue excessive strain. Toluidine Blue stain. (For interpretation of the references to color in this figure legend, the reader is referred to the web version of the article.)

that approximate the inner diameter of the implant threads [16] (Fig. 1). At early time points, an almost continuous bone-implant interface renders the system implant primary stability. At this stage, microcracks depicting that the yield strength of bone has been exceeded due to high stress levels are visualized along with initial remodeling taking place between the implant threads due to compression necrosis. As time elapses *in vivo*, an extensive remodeling region is evident presenting void spaces partially filled by newly formed bone [16]. Thus, the scenario that has been histologically observed in multiple instances confirms the theoretical and experimental basis [32,33] for the initial stability rendered by mechanical interlocking between implant and bone that at some point in time after placement under stable conditions decreased due to extensive bone resorption (Fig. 1). Subsequently, the resorbed area will be altered by newly formed woven bone, which eventually reestablishes the contact to the implant interface (secondary stability), and will subsequently remodel multiple times toward a lamellar configuration that will support the metallic device throughout its lifetime [35–41] (Fig. 1).

2.2. Intramembranous-like healing pathway (healing chamber osseointegration)

The second osseointegration pathway concerns the opposite scenario of the tight fit screw type implant, where void spaces between the implant bulk and the surgically instrumented drilled site walls are formed [42]. These void spaces left between bone and implant bulk, often referred as healing chambers, will be filled with blood clot immediately after placement and will not contribute to primary stability . These however, have been regarded as a key contributor to secondary stability [23,43].

The early healing biology and kinetics of bone formation in healing chambers has been discussed in detail by Berglundh et al. [42] while the effect of healing chamber size and shape on bone formation has been explored elsewhere [43,44]. Such healing chambers, filled with the blood clot, will evolve toward osteogenic tissue that subsequently ossifies through an intramembranous-like pathway [42]. Noteworthy is that unlike the interfacial remodeling healing pathway, healing chamber configurations do not encompass the initial cleanup process due to microcracking and ostecompression [22, 42,44]. In this case, the blood filling the space between pristine bone and device will develop toward a connective tissue network that provides a seamless pathway for cell migration within the space once filled by the blood clot (Fig. 2). Such healing configuration thus allows new bone formation throughout the healing chamber from all available surfaces (implant surface, instrumented bone surface) and within the chamber volume. Thus, intramembranous-like healing mode presents substantial deviation from the classic interfacial remodeling healing pathway observed in tight fit screw-type implant [21, 41,43].

2.3. The hybrid healing pathway: bringing together interfacial remodeling and intramembranous-like bone healing modes

Recent investigations have employed either experimental implant designs with an outer thread design that provided stability while the inner thread and osteotomy dimensions allowed healing chambers [42,45,46] or alterations in osteotomy dimensions in large thread pitch implant designs [22,47,48]. The rationale for these alterations lie upon the fact that thread designing may allow for both high degrees of primary stability along with a surgical instrumentation outer diameter that is closer to the outer diameter of the implant allowing healing chamber formation. Since healing chambers allow rapid intramembranous-like rapid woven bone formation [49], such rapid bone growth may compensate for the implant stability loss due to compression regions where implant threads contacts bone for primary stability (Fig. 3).

While promising developments have been made over the last five decades regarding implant hardware designing and how it dictates bone healing and long-term bone morphology around endosteal implants, it is widely recognized that other design features do in fact hasten osseointegration and can further increase the performance of implant hardware [11]. For instance, lower length scale design parameters have been designed in an attempt to change the degree of intimacy between host biofluids and implant surface while also changing cell phenotype to hasten biological response [50–53]. However, their early effects are directly related to their strategic hierarchical placement as a function of implant hardware design since healing mode and kinetics drastically shift as a function of the macrometer scale variables. It is thus

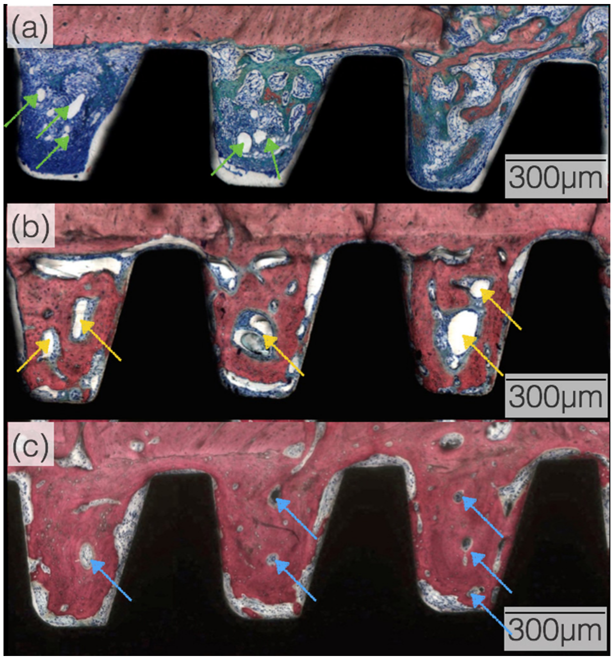

Fig. 2 – Stevenel's blue Von Giesson's stained optical micrographs of healing chamber implants (intramembranous healing mode) in a beagle dog model. (a) At 3 weeks *in vivo*, the surgical instrumentation line is evident forming the healing chambers that are filled with osteogenic tissue presenting initial bone formation (osteoid stained in green, bone stained in red) from the instrumentation line toward the center of the chamber, within the healing chamber volume, and from the implant surface toward the central region of the chamber. Initial revascularization is depicted by green arrows. (b) At 6 weeks *in vivo*, the healing chambers are filled from bone that originated form the surgical instrumentation and implant surfaces along with bone formed within the healing chamber. The yellow arrows depict spaces occupied by blood vessels forming the primary osteonic structures better defined at (c) 12 weeks, where the primary osteonic structures are depicted by blue arrows. (For interpretation of the references to color in this figure legend, the reader is referred to the web version of the article.)

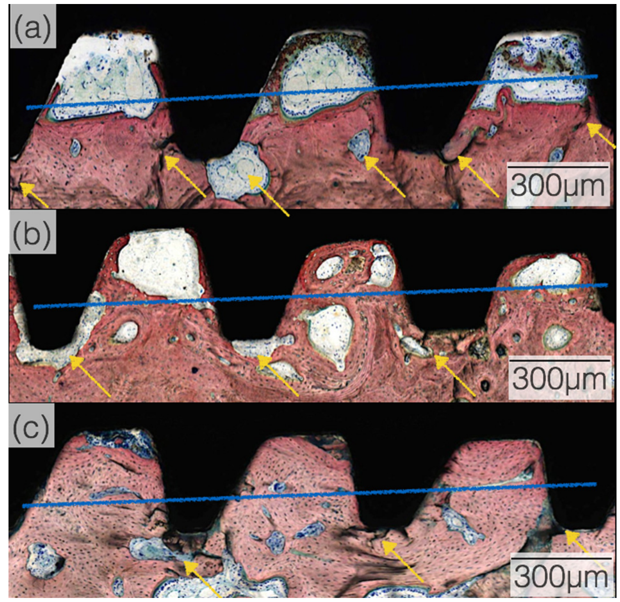

Fig. 3 – Stevenel's blue Von Giesson's stained optical micrographs of implants in bone representing the hybrid healing pathway in a beagle dog model. (a) At 3 weeks *in vivo*, the surgical instrumentation line has retracted from its estimated location (blue line) and is forming the healing chambers that are filled with osteogenic tissue presenting initial bone formation (osteoid stained in green, bone stained in red) from the instrumentation line toward the center of the chamber, within the healing chamber volume, and from the implant surface toward the central region of the chamber. Note the extensive micro cracking and the initial interfacial remodeling taking place at regions where the implant outer thread diameter was larger than the osteotomy diameter (yellow arrows). This interfacial remodeling is still evident at (b) 6 weeks (yellow arrows), where higher degrees of healing chamber filling is observed due to new bone formation occurring from the surgical instrumentation and implant surfaces along with bone formed within the healing chamber. (c) At 12 weeks, interfacial remodeling is nearly complete and an intimate interface between bone at the remodeling regions is under establishment with the implant surface (remodeling regions and micro cracks depicted by yellow arrows), and higher degrees of filling are observed within the healing chamber. (For interpretation of the references to color in this figure legend, the reader is referred to the web version of the article.)

intuitive that implant hardware should be strategically designed to allow adequate implant primary stability while maximizing interaction between the host biofluids and implant surface. For instance, the reduced length scale design features intended to improve the establishment and maintenance of continuous pathway for bone forming cell migration toward the implant surface will not be as efficient in accelerating osseointegration in regions where cell-mediated interfacial remodeling initially occurs after placement due to initial hardware design interaction with bone. Thus, implant hardware designs that allow healing chamber formation are more suited to deliver adequate conditions for improved micrometer and the nanometer length scale design features performance in hastening early osseointegration.

3. The effect of implant microgeometric designing in bone healing: a prelude to nanometer scale designing

One of the most researched areas, and one that has had significant impact on treatment strategies, is unquestionably the implant surface engineering. Over the years, surface topography modification has been attempted through various methodologies, and dramatic changes in osseointegration quality and quantity have been witnessed. The primitive surface finish of the osseointegrated implants proposed was that of turned implants manufactured by a machining process. These turned (machined) implants (better known as Brånemark-type implants) dominated the market until the mid-1990s and therefore, have the longest clinical documentation [4,54]. From such long-term clinical evidences, it can be concluded that turned implants present a clinically acceptable prognosis, if the traditional healing protocol (2-stage approach with a healing period of 3 months in the mandible, and 6 months in the maxilla) is followed [55], with a baseline assumption that the implant sites were fully healed ridges with good bone quality.

Although successful from a long-term perspective, the indications for turned implants were limited to healthy subjects with sufficient bone, and the treatment period created discomfort for the patients. Thus, the central focus and motivation for further surface topography research have been to shorten the time to osseointegrate and to expand the clinical modalities. As a result, some implants with extremely rough surface topography were developed and have been circulated in the market for some years, based on the simple engineering concept that rougher surfaces would provide mechanically higher interlocking between surface and the bone.

One of the methods commonly used to roughen the implant surface was the titanium plasma spray (TPS) technique, which yielded a bumpy surface configuration with extremely high average (mean) height deviation (R_a of 4–5 μm) as compared to the turned Brånemark-type implants. In preclinical investigations, such extremely rough surface topography of the TPS surface presented improved osseointegration compared to the turned surfaces [56–58]. Unfortunately, the clinical trials seemed to present little or rather negative outcomes with progressive marginal bone loss [59–66], resulting in TPS-roughened implant surfaces falling from favor among implant manufacturers.

From the mid-1990s to date, it has been experimentally demonstrated that osseointegration is improved and accelerated through various roughening procedures [67,68], such as sand blasting [69–71], acid etching [72–74], anodic oxidation [75–77], and even laser etching [67,68,78–80], and that there exists an optimal range in the micrometer scale [81]. The so-called moderately microroughened implant surfaces have been proven to present improved osseointegration in experimental and in clinical studies [82,83]. Today, implant surfaces with moderately textured microtopographies (S_a 1–2 μm) provide a basis for the majority of commercially available implants. Turned implants as a substrate are treated with the aforementioned procedures, strategically roughening them at the micrometer length scale to present improved bone response.

Owing to the improved osseointegration proven in experimental studies, it is now believed that the amount of time needed to establish implant–bone system biomechanical competence for functional load bearing can be significantly reduced [84]. Based on this experimental evidence, alteration in the clinical loading protocol (from delayed to early or immediate) has been attempted, presenting long-term clinical success [85]. It must be noted that the dramatic transition in clinical loading protocol results from the combined effect of numerous factors and, strictly speaking, cannot be attributed solely to the microroughened surface topography. Thus, although manufacturers commonly claim that a newly developed implant surface can reduce the time needed to osseointegrate, one must keep in mind that osseointegration is an outcome of the combination of different designs [86].

However, microtopography undoubtedly influences improved clinical success, especially in compromised situations such as poor-quality bone, or irradiated bone. It has been reported by Khang et al., in a multicenter study comparing the success of turned *versus* dual acid-etched surfaces in poor bone quality sites, that the clinical success was significantly higher for the moderately roughened implants than the turned implants [87]. This is in accordance with the report from Pinholt stating that the survival of moderately roughened implants was significantly higher compared to that of turned implants in grafted maxillary bone sites [88]. Even in post-tumor-resected irradiated sites, implant survival is dramatically higher for moderately roughened implant surfaces than for turned surfaces after 5 years in function [89], which indicates that treatment using moderately roughened implants significantly improved postoperative quality of life for patients who undergo massive oral and maxillofacial resection therapy.

In the space of a mere decade, implant surface modification has advanced to a new stage with the introduction of so-called nanolevel modification [18,90]. The nanolevel modification of implant surfaces, normally impossible to detect unless adequate instrumentation is employed, is based on the knowledge that the application of nanostructures (less than 100 nm in size in at least one dimension) significantly upregulate the biologic responses, since elements such as growth factors, proteins, and cells interact at this level [91–94].

It has been reported that the nanostructured surface is *bioactive*, that is, it has the potential to cause a reaction in the living body, whereas it is well known that the titanium or the titania itself is a *bioinert* material, and thus has no such potential [95]. Material bioactivity is one of the core concepts of the biologically inspired biomimetic engineering, which is a cross-link between material science and tissue engineering/regenerative medicine. The nanometer length scale modification has recently received significant attention in the interest of increased bioactivity.

4. The nanometer scale designing: current techniques and trends

While the macrometer and micrometer implant design parameters have been investigated over several decades, endosteal implant designing at the nanometer length scale is relatively new and its recent developments are hereafter presented in an objective fashion.

The nanometer scale was likely ‘born’ as early as when matter itself came into existence at the Big Bang. The universe as we see it is in the macrometer scale (1–1000 m); however, it can be drilled down to the invisible universe, to the micrometer scale (10^{-3} m) and further down to the nanometer scale (10^{-9} to 10^{-6} m, *i.e.* 1–1000 nm), where the building blocks of the universe, the atom and the sub-atomic particles (protons, neutrons, and electrons) interact electromagnetically. At the time of its origin, the Earth's matter in the nanometer scale comprised of inorganic particles of solidified core. Billions of years later, organic, biological molecules with various degrees of organization appeared, and started to interact with the inorganic components of the planet at various scales, resulting in complex inorganic–organic systems. The nanometer scale is quintessential to the function of these systems [96].

While it is obvious that the nanometer scale can be utilized for multiple engineering purposes, the reduced dimensions confer unique properties to the materials fabricated with nanotechnology (especially at 1–100 nm, which defines the grain size of such materials) and this has attracted significant interest in the research community. From a physical standpoint, nanoparticles are small enough to interact with DNA, which is approximately 2 nm in diameter [97].

The physical principles governing materials science in the macro- and micrometer scale have been exploited in the past, in the analysis of quantum mechanical relationships, which led to the development of novel fields, such as condensed matter physics (especially solid-state physics), statistical mechanics, and thermodynamics. Although these quantum mechanical relationships have been experimentally validated by material scientists, modern manufacturing techniques for precise atomic buildup at the nanometer scale, have shown that materials with a reduced scale in at least one of their 3 dimensions exhibit substantially different electronic configurations as compared to their larger-scale counterparts. This phenomenon, described as *quantum confinement*, depends on the number of dimensions with the reduced scale (typically <100 nm) in the *xy*, *xz*, and *yz* planes. In short, an alteration in electronic configuration based on the number of atoms contributing to the reduced-scale domains has facilitated substantial advances in the understanding of matter. This property has been well received by the material science community and is currently being developed for a variety of applications [98].

With regard to implant surfaces and nanomaterials, the possibilities are limitless, as nanoscale fabrication methods are becoming widely available. Nanotechnology-based manufacturing processes can alter the texture, length, scale and pattern of implant surfaces, while at the same time altering the chemical properties of the substrate by means of quantum confinement [94].

From a general perspective, recent research strongly suggests that alterations in surface topography can lead to changes in surface chemistry. Such phenomena may be intensified when features at the nanometer scale are considered. Not surprisingly, nanoscale features presenting both short- and long-range ordering have been shown to alter various aspects of cell behavior and are the subject of active research [99].

For instance, if one considers nanotopographical texturing of a surface, an exponential increase in surface area is expected along with alterations in surface electronic properties, due to the formation of nanoscale peaks, by virtue of 2-dimensional confinement. Thus, it is expected that the surface energy, resulting from nanotopographical texturing, will deviate from both smooth and microscale texturing. An increase in surface energy arises not only due to

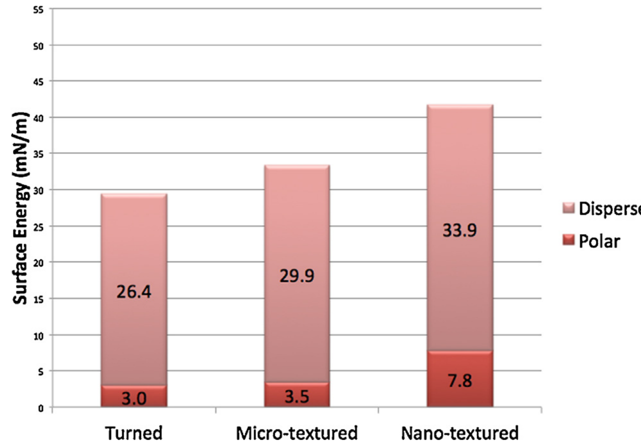

Fig. 4 – Surface energy measured by the OWRK method of turned, micro-textured, and nano-textured Ti–6Al–4V substrates.
(*Source*: Paulo G. Coelho's laboratory archives).

alterations in surface roughness, unevenness, and branching level (represented by the dispersed component contribution), but also due to alterations in surface chemistry, the presence of polar groups, electric charges, and free radicals (represented by the polar component contribution) when using the reduced scale rendered by nanotopography [100] (Fig. 4). The Owens–Wendt–Rabel–Kaelble approach [101,102] is a common method for calculating the surface energy [103]. In essence, droplets of purified water, ethylene glycol, and methylene iodide are separately used for the calculation of surface energy due to their wide range of intermolecular forces, non-toxicity, high surface tension, and known specific polarities [104]. Surface energy is calculated as follows:

$$\gamma_L = \gamma_L^D + \gamma_L^P \quad (1)$$

where γ_L is the surface energy, γ_L^D the disperse component, and γ_L^P the polar component. Previous studies considering nanoscale and microscale topographies have demonstrated improved wettability at the nanoscale surface [105]. This may be because the surface area significantly increases with nano-level surface modifications, and on many occasions the surface is negatively charged [105]. Thus, due to both physical and chemical features inherent to the nanometer scale, such surfaces have been known to affect cell behavior.

The positive effect of surfaces presenting nanoscale features, on the adhesion, spreading, motility, proliferation, adhesion selectivity, and differentiation of osteoblasts has been previously reported [90,106–109], showing unequivocal evidence that certain cellular phenomena can be triggered through nanometer length-scale modifications. Therefore, it is proposed that such modifications should be incorporated into dental implants designed to hasten osseointegration.

From the perspective of a hierarchical implant design, the hardware and microgeometry/topography are intended not only to provide the device primary stability through mechanical engagement and an increase in friction between implant and bone, respectively, but also to allow adequate bone-healing conditions, where substantial interactions exist between blood clots and the implant surface, immediately after the placement of the implant [22]. While implant hardware and microscale modifications will dictate tissue-level interaction and the peri-implant wound-healing cascades around the implant [22,23,42,44], nanoscale features present a potential to boost osteoblastic behavior, and thus hasten osseointegration. However, although *in vitro* cell culture studies demonstrated positive effects of nanoscale features on osteoblastic cells [110–112], any direct translation of such nanoscale features to implants, without considering implant hardware characteristics and microscale design parameters, may be misleading. Such contradictions resulted in the established rationale for hierarchical placement of nanoscale features within microscale texturing when designing dental implant surfaces. This strategy facilitates adequate intimate interaction between the blood clot and implant surface, so that osteogenic cells may travel through a seamless pathway toward the device surface, and once there, to be further altered in phenotype by nanoscale features. Applying this design guideline, implant surfaces presenting nanoscale texture and chemistry alteration have been manufactured.

Reduced-scale manufacturing techniques have been compiled in engineering literature and are beyond the scope of this review. From a manufacturing perspective, many, if not all, of the available techniques may be utilized for patterning implant surfaces with nanoscale features [97]. However, since high throughput is necessary for economically viable manufacture of implant surfaces, industrial methods for nanoscale surface modification are restricted to a few additive and subtractive techniques. To date, 4 representative implant surfaces presenting nanoscale features have been made commercially available. It must be acknowledged that implant surfaces other than the ones made commercially available under the “nano” label have been also characterized to present nanometer scale features. For example, TiUnite (Nobel Biocare, Zurich, Switzerland), SLActive (Institut Straumann, Basel, Switzerland) and OsseoSpeed (Dentsply IH, Mölndal, Sweden), originally not presented by their respective manufacturers as surfaces presenting nanometer scale features, indeed present nanometer scale surface patterning [84,113,114].

Of the commercially available nanometer scale surfaces claimed to be “nano” by their manufacturers, 2 contain surface modifications, such as bioactive, calcium-and-phosphate components, manufactured through subtractive followed by additive methods; the other 2 are manufactured mainly through subtractive processes. The nanoscale surfaces presenting bioactive ceramic components were both named NanoTite™ by their respective manufacturers (Bicon LLC, Boston, MA, USA; Biomet 3i, Palm Beach Gardens, FL, USA). While their final physicochemical configurations are distinctively different, both surfaces are manufactured by an initial subtractive method prior to their divergent additive methods. For the Bicon surface, a 20–50-nm-thick ion beam assisted deposition (IBAD) of calcium phosphate (CaP) results in the coating of a moderately rough microtextured substrate obtained by alumina blasting/acid etching (AB/AE) [115]. In the case of Biomet 3i surface, Discrete Crystalline Deposition (DCD™), deposition of nanoscale CaP particles onto the textured, acid-etched surface is performed *via* a sol–gel process. Previous work has demonstrated that the particle component covered approximately 50% of the surface [16]. Although both surfaces presented bioactive components, their purpose, and intended coating kinetics *in vivo* differed substantially.

The rationale for the IBAD of 20–50-nm-thick, mainly amorphous coating onto the AB/AE-microtextured surface was to leverage the highly osteoconductive properties of CaP, while avoiding issues presented by thick plasma-sprayed hydroxyapatite (PSHA) coatings, where long-term performance is highly dependent on implant hardware configuration [116]. In short, the rationale was to expose the healing site to bioactive calcium phosphate elements with the known osteogenic properties and simultaneously benefit from complete dissolution/resorption of the IBAD coating due to its amorphous nature. This would result in intimate contact between bone and the AB/AE-microtextured surface. Biomet 3i’s technique for incorporation of nanoscale features on the other hand, was intended to increase substrate osteoconductivity with the help of multiscale (micro- and nano-) texture levels and the chemical composition rendered by the DCD method.

The remaining 2 surfaces presenting nanoscale features are both manufactured by subtractive methods [11]. The first OsseoSpeed™ (Astra Tech AB, Mölndal, Sweden), (OSP), requires a titanium oxide blasting procedure, which renders a micrometer-level texture to the surface, followed by a hydrofluoric acid etching procedure, which results in a nanoscale texture within the microscale texture. The second, Ossean™ (Intra-Lock International, Boca Raton, FL, USA) (OSS) is fabricated by robotic microblasting of a resorbable blasting media (RBM) powder that results in nanoscale topography simultaneously within a larger-scale microtopography. Regardless of the fabrication method, no long-range ordering of the nanoscale features is obtained [11,117].

Despite the substantially different fabrication methods, from a topographical standpoint, all 4 surfaces present nanotexture within microtexture surface features. From a surface chemistry standpoint, the IBAD-fabricated surface presents primarily Ca, P, and O in its surface, since it has a uniform coating with nanometer-scale thickness, whereas the DCD surface presents elements from bioactive ceramic and substrate components [16,118]. Minute quantities of fluoride have been detected along with substrate alloy components in the case of OSP [119], whereas bioactive ceramic is found along with substrate alloy elements on the OSS surface [120].

Despite recent introduction, substantial advances have been achieved with nanometer scale materials in the area of implant surfaces. Previous studies investigating the biological response to nanoscale surfaces were funded by manufacturers and often utilized their predecessor surfaces as control groups. A series of studies have followed, where different nanoscale surfaces have been compared.

4.1. *Cell culture studies*

The IBAD surface was evaluated in 3 different cell culture studies, where it was compared to its AB/AE uncoated substrate and as-machined surfaces [121–123]. The first study, conducted with primary human osteoblasts, presented mixed results with the IBAD and AB/AE surfaces regarding osteogenesis-related events [121]. The second study was intended to evaluate the effect of the same 3 surfaces on human osteogenic cells, peripheral blood mononuclear cells (PBMC), and osteogenic cells cocultured with PBMC without exogenous stimuli. Relative differences in results were generally observed among surfaces for the 3 different cultures (always favoring the IBAD and AB/AE surfaces over the as-machined control); however, the "multi-cell type" interactions had a more pronounced influence on the *in vitro* cellular events related to initial stages of bone formation than did the surface texture or chemistry [123]. Finally, the third study evaluated the same 3 surfaces in a culture of human polymorphonuclear neutrophils (PMNs). The results showed that the addition of a thin CaP coating to the AB/AE surface influenced the secretion profile of proinflammatory cytokines [122]. Taken together, these cell culture studies comparing IBAD, AB/AE, and turned surfaces presented mixed results that demonstrated substantial disagreement with *in vivo* preclinical results for the same surfaces, as subsequently discussed.

The DCD surface has been evaluated in primary mouse alveolar bone cells relative to OSP, TiUnite® (Nobel Biocare, Kloten, Switzerland), and SLA® (Straumann, Basel, Switzerland) surfaces [124]. Following a 48-h culture, the OSP and SLA surfaces displayed the highest degrees of cell adhesion. The DCD surface presented significantly lower degrees of cell confluence relative to the 3 other surfaces [124].

The OSP surface has been compared to its titanium oxide blasted predecessor, TiOblast (Astra Tech), in a mouse pre-osteoblast MC3T3-E1 cell culture model [125]. The results showed no differences in cell viability and proliferation, but OSP showed more branched cell morphology compared to the control at 48 h. At 14 days, increased gene expression of IGF-I, BSP, and osterix were observed for the OSP surface, indicating that osteoblast differentiation and mineralization were affected by the nanoscale surface [125]. A more comprehensive real-time PCR study that considered bone-specific gene expression in the same 2 surfaces plus a turned control in a MC3T3-E1 cell culture model as well as in implant-adherent cells from a rabbit tibia model, all demonstrated that the OSP surface outperformed the control in osteogenic gene expression events [126]. Another study evaluating adherent mesenchymal stem cells on OSP and its predecessor presented favorable osteoinduction and osteogenesis of these cells for the OSP surface [127]. As previously mentioned, when OSP was compared to the DCD surface in a primary mouse alveolar bone cell culture model, superior results were observed for the OSP surface [124]. Masaki et al. also demonstrated that OSP altered cell behavior relative to other surfaces [69].

Cell culture studies considering the OSS surface also compared it to its microscale-textured predecessor [121]. In this study, cell adhesion, proliferation, and alkaline phosphatase activity were assessed with human SaOS-2 osteoblasts and bone mesenchymal stem cells in nonosteogenic culture conditions. The results demonstrated higher osteoblastic differentiation for the nanoscale surface relative to its microscale counterpart [121].

In general, cell culture studies depicted favorable results for nanoscale surfaces relative to their microscale predecessors. To date, no such predecessor comparison has been performed for the DCD surface, and the mixed results observed for the IBAD surface relative to the uncoated AB/AE substrate may have been related to the dissolution of the amorphous coating. Regarding OSP and OSS, where similar microlevel-textured surfaces were used as controls against nanoscale-within-microscale topography surfaces, it is unequivocal that the nanoscale features substantially altered cell behavior favoring osteogenic cellular events.

4.2. *Preclinical in vivo models*

Whereas mixed results were obtained for the IBAD surface in cell culture assays, a series of studies demonstrated its superiority to uncoated surfaces for both biomechanical and histometric outcomes [128–130]. For cylindrical implants with the IBAD surface, higher degrees of osteoconductivity were observed, along with higher degrees of biomechanical fixation at early implantation times, than for their uncoated counterparts [128–130]. Furthermore, it has been demonstrated that the coating thickness played a role in biomechanical results [129]. In larger preclinical *in vivo* models, significantly higher levels of bone-to-implant contact (BIC) and biomechanical fixation were observed when commercially available implants were utilized [115,118,131–133]. While significant improvements were consistently obtained relative to uncoated implants, studies that considered IBAD- *versus* PSHA-coated implants demonstrated that the PSHA-coated implants outperformed the IBAD-coated ones, especially with respect to biomechanical competence at early implantation times [118,129,132,134].

The DCD surface showed promising results in rodent models relative to its microscale-textured counterpart [135–137]. With the bone-healing chamber design in a rat model, higher degrees of bone ingrowth were observed [136], and higher degrees of bone adhesion were detected, when the pullout strength from the bone for the DCD-coated implants was compared to the predecessor control (regarded as bone bonding, due to the presence of nanoscale features on the implant surface) [135]. In a beagle canine model, however, in contrast to rodent models, no differences in bone response to either DCD or its predecessor surface were detected [138–141]. When the DCD surface was compared to other moderately rough surfaces in the more challenging scenario of immediate placement within extraction sockets, the DCD surface showed significantly lower BIC levels relative to a dual acid-etched surface, an SLA surface, and an anodized surface. When socket architecture was considered, no difference was detected among the 4 implant groups [142].

The OSP surface has also been well documented in laboratory preclinical animal models *versus* its moderately rough microscale-textured predecessor and other surfaces. Ellingsen et al. [18] demonstrated higher biomechanical competence and BIC levels for the OSP relative to its microscale predecessor (TiOblast, Astra Tech) in a rabbit tibia model. Through modification in the relationship between implant macrogeometry and surgical instrumentation (healing chambers between threads [23,42]), Berglundh et al. [119] demonstrated superior results for the OSP surface relative to its predecessor regarding the amount of bone formation within healing chambers.

In addition, the OSP surface has been compared to various other microscale surfaces in numerous preclinical laboratory animal models. In an *in vivo* rabbit model, the OSP surface presented significantly higher bone response at 2 weeks as compared to an anodized surface presenting micrometer-level texturing [143]. In a crestal bone maintenance study conducted in minipigs by Heitz-Mayfield et al. [144], both OSP and SLA implant surfaces presented higher degrees of crestal bone maintenance as compared to an implant having an anodized surface with micrometer-level texturing [144].

OSP has also been evaluated against other microscale-textured surfaces with enhanced surface wettability in fresh extraction sockets in beagle dogs [145]. No differences were detected in host-to-implant response up to 4 and 12 weeks. Another study comparing OSP to other surfaces in fresh extraction sockets failed to demonstrate differences among groups in all parameters evaluated [146]. It should be noted that this particular study primarily comprised of the evaluation of soft tissue measurement outcomes and not osseointegration measurements. However, bone maintenance around implants immediately placed in extraction sockets has been shown to influence soft tissue measurements [147,148].

Comparisons between the OSP surface and other nanoscale surfaces in numerous preclinical laboratory animal models are described below.

The OSS surface has also been well documented in comparison to its AB/AE predecessor in a series of preclinical *in vivo* studies. In the first, conducted by Marin et al. [149], OSS and AB/AE surfaces were histometrically and biomechanically evaluated in a beagle model. Although the group reported no significant differences in BIC between surfaces at both 2 and 4 weeks, a roughly 100% increase in removal torque was seen for the OSS surface relative to its predecessor, strongly suggesting that bone around the OSS surface presented higher mechanical properties [149]. Similar results were obtained by Marin et al. [150] where the OSS surface was compared to a dual acid-etched, moderately rough surface with micrometer-level texture.

In a protocol similar to that of Mendes et al. [135], who reported bone bonding between DCD nanoscale-modified surface and bone, Coelho et al. observed the same bonding phenomenon when the OSS surface was compared to its AB/AE microscale-textured counterpart. This suggested that bone bonding might also be achieved by the lower levels of Ca and P on the OSS implant surface (crystalline HA particles being present at much higher numbers for the DCD surface) [151]. Alternatively, the authors speculated that bone bonding to the OSS surface might have been due to the nanoscale texture, rather than the lower levels of Ca and P. To address this question of whether nanoscale texture or surface chemistry was responsible for the high osteoconductive properties of the OSS surface, Coelho et al. tested an implant with a nanoscale texture similar to that of the OSS surface but produced through silica blasting, so that Ca and P were not present on its surface [152]. When these were compared *in vivo* in a beagle model, no differences in bone response (torque and BIC) were detected, strongly suggesting that the nanotopographical component of the OSS surface played a larger role in its osseointegration than low levels of Ca and P [152]. Experimental studies should be conducted to further address the relative contributions of nanoscale texture and surface chemistry to the bonding of bone to implant surfaces [151]. Another histometric, nanomechanical, and gene expression study conducted in a rodent model unequivocally showed higher BIC, bone mechanical properties (hardness and modulus of elasticity), and osteogenic gene expression for the OSS surface as compared to its predecessor, indicating that the nanoscale surface indeed modulates osteoblastic cell response, leading to faster osseointegration and bone mechanical property achievement [153]. Finally, the OSS surface, when evaluated in immediate extraction socket implants, was able to maintain higher levels of bone attachment at the buccal flange relative to implants presenting a smooth cervical region [154].

When compared to various microscale surfaces, OSS presented favorable biomechanical and histometric results. For instance, a study comparing the OSS surface to surfaces microscale-textured by AB/AE or RBM alone, by plasma treatment, or by RBM plus acid etching, depicted significantly higher torque levels for the OSS surface relative to others [70]. Another study, consisting of histometric and nanomechanical assessment of OSS *versus* OSP, SLA, anodized, and RBM surfaces, demonstrated higher BIC for OSS at the earliest time point *in vivo*, and slight but not significant differences in bone mechanical properties between surfaces [120].

The OSS surface was also compared to the DCD nanotextured surface and to 2 microscale-textured surfaces in a canine model at 10 and 30 days post-implantation [16]. All implant macrogeometries and surgical instrumentation used were the same, minimizing confounding osseointegration factors due to implant hardware. The OSS surface presented significantly higher biomechanical competence (assessed by removal torque) than the other groups at 30 days *in vivo* [16].

One study directly comparing the biomechanical performance of OSS, OSP, and DCD implants has been reported, where the implants were placed in the beagle mandible at 1 and 3 weeks *in vivo* prior to euthanasia. When torqued out, the OSS implants presented significantly higher removal torque values than the OSP and DCD implants. At 3 weeks, both OSS and OSP implants presented comparable results, and both were significantly higher than the DCD surface [155]. However, the results of this study must be interpreted with caution, as it compared the performance of the 3 different implant systems with nanoscale surfaces and not the performance of the 3 different surfaces on the same implant hardware. Specific to the removal torque results, it must be noted that the significant differences between groups may have been influenced by differences in implant hardware that possibly mitigated the effect at the nanometer scale on osseointegration.

4.3. *Clinical evidence*

Outcomes of a few published clinical trials regarding some implant surfaces with nanotopography are described in this section and summarized in Table 1. The DCD surface has been evaluated in a prospective 1-year clinical study on immediate loading with tapered implants placed in 42 patients, with 55% located in the posterior region (20 single crowns [SC], 30 fixed dental prostheses [FDP], and 7 full-arch [FA] maxillary reconstructions). Survival rate at 1 year was 99.4% [156]. The same surface had earlier been evaluated in a prospective 1-year clinical study with immediate loading using different macrogeometry (Prevail®). There, 35 patients received 102 implants

Table 1 – Clinical outcomes of prospective studies of implant surfaces presenting nanotopography.

Author/implant surface	Prostheses design	Survival rate (%)	Observation period	Immediate occlusal loading	Control group (non-nano-enabled surface)
Östman et al. [155]/DCD	20 SC, 30 FDP, 7 FA	99.4% (1 implant failure)	1 year	Yes	No
Östman et al. [156]/DCD	14 SC, 26 FDP, 4 FA	99.2% (1 implant failure)	1 year	Yes	No
Cecchinato et al. [157]/OSP	91 SC	Not described	3 years	Yes	No
Collaert et al. [158]/OSP	25 FA	100%	2 years	Yes	No
De Bruyn et al. [159]/OSP	132 SC	94–98%	3 years	No	No
Mertens and Steveling [84]/OSP	31 SC, 4 FDP, 1 FA	97%	5 years	Yes/early loading included	No
Mertens et al. [160]/OSP	Fixed and removable	97.85%	28 months	No	No
Noelken et al. [161]/OSP	SC and FDP	100%	2 years	No	No
Raes et al. [162]/OSP	SC	98%	1 year	Yes	No

Abbreviations: DCD, discrete crystalline deposition™; OSP, OsseoSpeed™; SC, single crown; FDP, fixed dental prostheses; FA, full-arch.

(65% in the posterior region), to support 14 SC, 26 FDP, and 4 FA reconstructions. The survival rate was 99.2% (one implant failure) [157].

The following list consists of clinical studies evaluating the OSP implant surface:

1. Immediate loading for soft tissue long-term (3 years) evaluation, where 93 patients were treated with 93 implants [158].
2. Immediate loading of 125 implants placed to support full-arch rehabilitations, followed-up prospectively for 2 years with a survival rate of 100% [159].
3. Immediate provisionalization (no centric or eccentric occlusal contact) of 132 implants supporting single anterior maxillary crowns (62 placed in extraction sockets, 70 in healed sites), with survival rates of 94.5% and 98.3% [160].
4. 17 patients receiving 33 implants in the maxilla and 16 in the mandible to support SC, FDP, or FA restoration [85].
5. 15 patients receiving 99 implants at 19 different intraoral recipient sites (15 in the maxilla, 4 in the mandible), previously grafted with calvarial split grafts, and loaded after 3 months with fixed and removable prostheses, with a 28-month follow-up showing an implant survival rate of 97.85% [161].
6. 37 implants immediately placed and provisionalized, without occlusal contact, with SC and FDP, where 17 replaced central incisors, 9 lateral incisors, 6 canines, and 5 premolars, presenting a 2-year survival rate of 100% [162].
7. 48 patients receiving single implants, immediately loaded after either conventional implant placement, immediate placement, or site grafting, with a prospective follow-up after 1 year of function indicating a 98% survival rate [163].

The studies described above and in the table shows that a combination of treatment concepts is commonplace, even within a single study: immediate and early loading; placement into grafted and nongrafted sites; varied prosthesis type and design, including single crowns, FDP, removable, and full-arch prostheses, screw- or cement-retained, with various implant diameters and lengths; and placement in different areas in the mouth (anterior or posterior, maxilla or mandible). Comparative efforts among studies, even for the same implant surface, are clearly a heuristic task. Of remarkable interest is that none of the studies that investigated the clinical outcomes of implants with nanolevel surface alterations included a control (*i.e.* same turned implant macro design without the nano-enabled features) for sound observation of the real impact of nanofeatures in immediate, early, and long-term clinical results. It must be emphasized that the nanometer scale component of the present review primarily concerns what has been made commercially available; a plethora of nanoscale surface modifications for bone-healing modulation are currently under development and showing remarkable improvements, such as increasing bone-healing velocity while also resulting in higher bone mechanical properties [164]. Such features are of utmost importance if challenging loading protocols are to be common practice and not utilized solely in selected cases.

4.4. *Nanotechnology: perspectives and challenges in implant dentistry*

A 2004 report on the market share of nanotechnology-enabled products emphasized that nanotechnology represents a "value chain" and not an industry or sector *per se*. In that report, revenue projections for 2014 had nanotechnology representing "4% of general manufactured goods, 50% of electronics and IT [information technology] products, and 16% of goods in healthcare and life sciences." Ten years ago, the revenues for products incorporating nanotechnology were approximately USD 13 billion, with roughly USD 8.5 billion coming from automotive and aerospace applications. Revenue rise for 2014 was projected to USD 2.6 trillion, with 2010–14 being a period when nanotechnology would become significant in pharmaceuticals and for medical devices, considering that lengthy, well-designed randomized controlled clinical trials (RCT) would by then have been able to demonstrate that nano-enabled materials substantially altered the nature of a product and its host response [165]. Obviously, this does not seem to be the case in implant dentistry, not only because RCTs comprising a substantially large patient pool, standardized prosthesis design, and implants both with and without nanostructural features are not available, but also because the multifaceted success criteria in implant dentistry are commonly not acknowledged [166]. A large gap between the promise of nanotechnology and its integration into a new generation of nano-enabled products is remarkably evident [167].

5. Concluding remarks

It is unequivocal that implant hardware does affect bone-healing pathways and that this may increase the micro- and nanolevel contribution to osseointegration. There is also an immense amount of published work supporting that micrometer scale surface modifications favor osseointegration by facilitating early host-to-implant response through tissue healing that facilitates cell migration and also shifts cell phenotype.

Since it has been experimentally determined that all length scale implant design levels substantially contribute to the osseointegration process, the biggest challenge for the future is to optimize the velocity and properties of these implants through adequately designed studies. It is worth noting that the word "optimization" is rarely used in the health sciences as it is in the physical sciences and mathematics, where it usually denotes that the contribution of every known variable related to a phenomenon (alone or in groups) has been experimentally determined and that mathematical inferences can be drawn to maximize outcome. Given the inconsistencies hitherto encountered in the implant literature, a substantial amount of work is warranted to ensure the adequate collection of data that will actually enable the optimization of osseointegration. Upon the completion of such germane series of studies, the macro-, micro-, nano-scale design components will be entirely able to work in tandem.

Acknowledgments

All authors equally contributed to the manuscript. The authors would like to express their gratitude to all their collaborators and students, who are the body and soul of the work presented in this review.

REFERENCES

[1] Bothe RT, Beaton LE, Davenport HA. Reaction of bone to multiple metallic implants. Surg Gynecol Obstet 1940;71(6):598–602.

[2] Leventhal GS. Titanium, a metal for surgery. J Bone Joint Surg Am 1951;33-A:473–4.

[3] Branemark PI, Hansson BO, Adell R, Breine U, Lindstrom J, Hallen O, et al. Osseointegrated implants in the treatment of the edentulous jaw. Experience from a 10-year period. Scand J Plast Reconstr Surg Suppl 1977;16: 1–132.

[4] Adell R, Lekholm U, Rockler B, Branemark PI. A 15-year study of osseointegrated implants in the treatment of the edentulous jaw. Int J Oral Surg 1981;10:387–416.

[5] Albrektsson T, Johansson C. Osteoinduction, osteoconduction and osseointegration. Eur Spine J 2001;2(10 Suppl.):S96–101.

[6] Barber AJ, Butterworth CJ, Rogers SN. Systematic review of primary osseointegrated dental implants in head and neck oncology. Br J Oral Maxillofac Surg 2011;49:29–36.

[7] De Bruyn H, Van de Velde T, Collaert B. Immediate functional loading of TiOblast dental implants in full-arch edentulous mandibles: a 3-year prospective study. Clin Oral Implants Res 2008;19:717–23.

[8] Shigehara S, Ohba S, Nakashima K, Takanashi Y, Asahina I. Immediate loading of dental implants inserted in edentulous maxillas and mandibles: 5-year results of a clinical study. J Oral Implantol 2014, http://dx.doi.org/10.1563/aaid-joi-D-14-00018. Apr 7. [Epub ahead of print].

[9] Vervaeke S, Collaert B, De Bruyn H. The effect of implant surface modifications on survival and bone loss of immediately loaded implants in the edentulous mandible. Int J Oral Maxillofac Implants 2013;28:1352–7.

[10] Vandeweghe S, Nicolopoulos C, Thevissen E, Jimbo R, Wennerberg A, De Bruyn H. Immediate loading of screw-retained all-ceramic crowns in immediate versus delayed single implant placement. Int J Prosthodont 2013;26:458–64.

[11] Coelho PG, Granjeiro JM, Romanos GE, Suzuki M, Silva NR, Cardaropoli G, et al. Basic research methods and current trends of dental implant surfaces. J Biomed Mater Res B Appl Biomater 2009;88:579–96.

[12] Browaeys H, Dierens M, Ruyffelaert C, Matthijs C, De Bruyn H, Vandeweghe S. Ongoing crestal bone loss around implants subjected to computer-guided flapless surgery and immediate loading using the All-on-4® concept. Clin Implant Dent Relat Res 2014, http://dx.doi.org/10.1111/cid.12197. Jan 8. [Epub ahead of print].

[13] Deporter DA, Kermalli J, Todescan R, Atenafu E. Performance of sintered, porous-surfaced, press-fit implants after 10 years of function in the partially edentulous posterior mandible. Int J Periodontics Restorative Dent 2012;32:563–70.

[14] Giro G, Tovar N, Marin C, Bonfante EA, Jimbo R, Suzuki M, et al. The effect of simplifying dental implant drilling

sequence on osseointegration: an experimental study in dogs. Int J Biomater 2013;2013:230310.
[15] Yeniyol S, Jimbo R, Marin C, Tovar N, Janal MN, Coelho PG. The effect of drilling speed on early bone healing to oral implants. Oral Surg Oral Med Oral Pathol Oral Radiol 2013;116:550–5.
[16] Bonfante EA, Granato R, Marin C, Jimbo R, Giro G, Suzuki M, et al. Biomechanical testing of microblasted, acid-etched/microblasted, anodized, and discrete crystalline deposition surfaces: an experimental study in beagle dogs. Int J Oral Maxillofac Implants 2013;28: 136–42.
[17] Jimbo R, Tovar N, Marin C, Teixeira HS, Anchieta RB, Silveira LM, et al. The impact of a modified cutting flute implant design on osseointegration. Int J Oral Maxillofac Surg 2014;43(7):883–8.
[18] Ellingsen JE, Johansson CB, Wennerberg A, Holmen A. Improved retention and bone-to-implant contact with fluoride-modified titanium implants. Int J Oral Maxillofac Implants 2004;19:659–66.
[19] Coelho PG, Teixeira HS, Marin C, Witek L, Tovar N, Janal MN, et al. The in vivo effect of P-15 coating on early osseointegration. J Biomed Mater Res B Appl Biomater 2014;102:430–40.
[20] Chowdhary R, Halldin A, Jimbo R, Wennerberg A. Influence of micro threads alteration on osseointegration and primary stability of implants: an FEA and in vivo analysis in rabbits. Clin Implant Dent Relat Res 2013, http://dx.doi.org/10.1111/cid.12143. Aug 27. [Epub ahead of print].
[21] Gottlow J, Barkarmo S, Sennerby L. An experimental comparison of two different clinically used implant designs and surfaces. Clin Implant Dent Relat Res 2012;14:e204–12.
[22] Coelho PG, Suzuki M, Guimaraes MV, Marin C, Granato R, Gil JN, et al. Early bone healing around different implant bulk designs and surgical techniques: a study in dogs. Clin Implant Dent Relat Res 2010;12:202–8.
[23] Leonard G, Coelho P, Polyzois I, Stassen L, Claffey N. A study of the bone healing kinetics of plateau versus screw root design titanium dental implants. Clin Oral Implants Res 2009;20:232–9.
[24] Coelho PG, Jimbo R. Osseointegration of metallic devices: current trends based on implant hardware design. Arch Biochem Biophys 2014;561C:99–108.
[25] Halldin A, Jimbo R, Johansson CB, Wennerberg A, Jacobsson M, Albrektsson T, et al. The effect of static bone strain on implant stability and bone remodeling. Bone 2011;49:783–9.
[26] Norton M. Primary stability versus viable constraint – a need to redefine. Int J Oral Maxillofac Implants 2013;28:19–21.
[27] Isidor F. Influence of forces on peri-implant bone. Clin Oral Implants Res 2006;17:8–18.
[28] Petrie CS, Williams JL. Comparative evaluation of implant designs: influence of diameter, length, and taper on strains in the alveolar crest. Clin Oral Implants Res 2005;16: 486–94.
[29] Huang H-L, Chang Y-Y, Lin D-J, Li Y-F, Chen K-T, Hsu J-T. Initial stability and bone strain evaluation of the immediately loaded dental implant: an in vitro model study. Clin Oral Implants Res 2011;22:691–8.
[30] Verborgt O, Gibson GJ, Schaffler MB. Loss of osteocyte integrity in association with microdamage and bone remodeling after fatigue in vivo. J Bone Miner Res 2000;15:60–7.
[31] Chamay A, Tschantz P. Mechanical influences in bone remodeling. Experimental research on Wolff's law. J Biomech 1972;5:173–80.
[32] Raghavendra S, Wood MC, Taylor TD. Early wound healing around endosseous implants: a review of the literature. Int J Oral Maxillofac Implants 2005;20:425–31.
[33] Gomes JB, Campos FE, Marin C, Teixeira HS, Bonfante EA, Suzuki M, et al. Implant biomechanical stability variation at early implantation times in vivo: an experimental study in dogs. Int J Oral Maxillofac Implants 2013;28:e128–34.
[34] Jimbo R, Sawase T, Shibata Y, Hirata K, Hishikawa Y, Tanaka Y, et al. Enhanced osseointegration by the chemotactic activity of plasma fibronectin for cellular fibronectin positive cells. Biomaterials 2007;28:3469–77.
[35] Mangano C, Perrotti V, Raspanti M, Mangano F, Luongo G, Piattelli A, et al. Human dental implants with a sandblasted, acid-etched surface retrieved after 5 and 10 years: a light and scanning electron microscopy evaluation of two cases. Int J Oral Maxillofac Implants 2013;28:917–20.
[36] Iezzi G, Piattelli A, Mangano C, Shibli JA, Vantaggiato G, Frosecchi M, et al. Peri-implant bone tissues around retrieved human implants after time periods longer than 5 years: a retrospective histologic and histomorphometric evaluation of 8 cases. Odontology 2012;102:116–21.
[37] Iezzi G, Vantaggiato G, Shibli JA, Fiera E, Falco A, Piattelli A, et al. Machined and sandblasted human dental implants retrieved after 5 years: a histologic and histomorphometric analysis of three cases. Quintessence Int 2012;43:287–92.
[38] Coelho PG, Bonfante EA, Marin C, Granato R, Giro G, Suzuki M. A human retrieval study of plasma-sprayed hydroxyapatite-coated plateau root form implants after 2 months to 13 years in function. J Long Term Eff Med Implants 2010;20:335–42.
[39] Coelho PG, Marin C, Granato R, Suzuki M. Histomorphologic analysis of 30 plateau root form implants retrieved after 8 to 13 years in function. A human retrieval study. J Biomed Mater Res B Appl Biomater 2009;91B:975–9.
[40] Piattelli A, Artese L, Penitente E, Iaculli F, Degidi M, Mangano C, et al. Osteocyte density in the peri-implant bone of implants retrieved after different time periods (4 weeks to 27 years). J Biomed Mater Res B Appl Biomater 2014;102:239–43.
[41] Davies JE. Understanding peri-implant endosseous healing. J Dent Educ 2003;67:932–49.
[42] Berglundh T, Abrahamsson I, Lang NP, Lindhe J. De novo alveolar bone formation adjacent to endosseous implants. Clin Oral Implants Res 2003;14:251–62.
[43] Marin C, Granato R, Suzuki M, Gil JN, Janal MN, Coelho PG. Histomorphologic and histomorphometric evaluation of various endosseous implant healing chamber configurations at early implantation times: a study in dogs. Clin Oral Implants Res 2010;21:577–83.
[44] Coelho PG, Granato R, Marin C, Teixeira HS, Suzuki M, Valverde GB, et al. The effect of different implant macrogeometries and surface treatment in early biomechanical fixation: an experimental study in dogs. J Mech Behav Biomed Mater 2011;4:1974–81.
[45] Abrahamsson I, Berglundh T, Linder E, Lang NP, Lindhe J. Early bone formation adjacent to rough and turned endosseous implant surfaces. An experimental study in the dog. Clin Oral Implants Res 2004;15:381–92.
[46] Abrahamsson I, Linder E, Lang NP. Implant stability in relation to osseointegration: an experimental study in the Labrador dog. Clin Oral Implants Res 2009;20:313–8.
[47] Campos FE, Gomes JB, Marin C, Teixeira HS, Suzuki M, Witek L, et al. Effect of drilling dimension on implant placement torque and early osseointegration stages: an experimental study in dogs. J Oral Maxillofac Surg 2012;70:e43–50.
[48] Bonfante EA, Granato R, Marin C, Suzuki M, Oliveira SR, Giro G, et al. Dual-acid-etched and as-machined implants

with healing chambers: an experimental study in dogs. Int J Oral Maxillofac Implants 2011;26:75–82.
[49] Witek L, Marin C, Granato R, Bonfante EA, Campos FE, Gomes JB, et al. Surface characterization, biomechanical, and histologic evaluation of alumina and bioactive resorbable blasting textured surfaces in titanium implant healing chambers: an experimental study in dogs. Int J Oral Maxillofac Implants 2013;28:694–700.
[50] Hamilton DW, Brunette DM. The effect of substratum topography on osteoblast adhesion mediated signal transduction and phosphorylation. Biomaterials 2007;28:1806–19.
[51] Leclercq L, Modena E, Vert M. Adsorption of proteins at physiological concentrations on pegylated surfaces and the compatibilizing role of adsorbed albumin with respect to other proteins according to optical waveguide lightmode spectroscopy (OWLS). J Biomater Sci Polym Ed 2013;24:1499–518.
[52] Yang D, Lu X, Hong Y, Xi T, Zhang D. The molecular mechanism of mediation of adsorbed serum proteins to endothelial cells adhesion and growth on biomaterials. Biomaterials 2013;34:5747–58.
[53] Zambuzzi WF, Coelho PG, Alves GG, Granjeiro JM. Intracellular signal transduction as a factor in the development of "smart" biomaterials for bone tissue engineering. Biotechnol Bioeng 2011;108:1246–50.
[54] Attard NJ, Zarb GA. Long-term treatment outcomes in edentulous patients with implant-fixed prostheses: the Toronto study. Int J Prosthodont 2004;17:417–24.
[55] Branemark PI, Adell R, Breine U, Hansson BO, Lindstrom J, Ohlsson A. Intra-osseous anchorage of dental prostheses. I. Experimental studies. Scand J Plast Reconstr Surg 1969;3:81–100.
[56] Schroeder A, Pohler O, Sutter F. Tissue reaction to an implant of a titanium hollow cylinder with a titanium surface spray layer. SSO Schweiz Monatsschr Zahnheilkd 1976;86:713–27.
[57] Simmons CA, Valiquette N, Pilliar RM. Osseointegration of sintered porous-surfaced and plasma spray-coated implants: an animal model study of early postimplantation healing response and mechanical stability. J Biomed Mater Res 1999;47:127–38.
[58] Gotfredsen K, Berglundh T, Lindhe J. Anchorage of titanium implants with different surface characteristics: an experimental study in rabbits. Clin Implant Dent Relat Res 2000;2:120–8.
[59] Vercaigne S, Wolke JG, Naert I, Jansen JA. The effect of titanium plasma-sprayed implants on trabecular bone healing in the goat. Biomaterials 1998;19:1093–9.
[60] Vercaigne S, Wolke JG, Naert I, Jansen JA. Histomorphometrical and mechanical evaluation of titanium plasma-spray-coated implants placed in the cortical bone of goats. J Biomed Mater Res 1998;41:41–8.
[61] Roccuzzo M, Aglietta M, Bunino M, Bonino L. Early loading of sandblasted and acid-etched implants: a randomized-controlled double-blind split-mouth study. Five-year results. Clin Oral Implants Res 2008;19:148–52.
[62] Mau J, Behneke A, Behneke N, Fritzemeier CU, Gomez-Roman G, d'Hoedt B, et al. Randomized multicenter comparison of 2 IMZ and 4 TPS screw implants supporting bar-retained overdentures in 425 edentulous mandibles. Int J Oral Maxillofac Implants 2003;18:835–47.
[63] Roynesdal AK, Ambjornsen E, Haanaes HR. A comparison of 3 different endosseous nonsubmerged implants in edentulous mandibles: a clinical report. Int J Oral Maxillofac Implants 1999;14:543–8.
[64] Roynesdal AK, Ambjornsen E, Stovne S, Haanaes HR. A comparative clinical study of three different endosseous implants in edentulous mandibles. Int J Oral Maxillofac Implants 1998;13:500–5.
[65] Astrand P, Anzen B, Karlsson U, Sahlholm S, Svardstrom P, Hellem S. Nonsubmerged implants in the treatment of the edentulous upper jaw: a prospective clinical and radiographic study of ITI implants – results after 1 year. Clin Implant Dent Relat Res 2000;2:166–74.
[66] Becker W, Becker BE, Ricci A, Bahat O, Rosenberg E, Rose LF, et al. A prospective multicenter clinical trial comparing one- and two-stage titanium screw-shaped fixtures with one-stage plasma-sprayed solid-screw fixtures. Clin Implant Dent Relat Res 2000;2:159–65.
[67] Wennerberg A, Albrektsson T, Johansson C, Andersson B. Experimental study of turned and grit-blasted screw-shaped implants with special emphasis on effects of blasting material and surface topography. Biomaterials 1996;17:15–22.
[68] Wennerberg A, Albrektsson T, Andersson B. Bone tissue response to commercially pure titanium implants blasted with fine and coarse particles of aluminum oxide. Int J Oral Maxillofac Implants 1996;11:38–45.
[69] Masaki C, Schneider GB, Zaharias R, Seabold D, Stanford C. Effects of implant surface microtopography on osteoblast gene expression. Clin Oral Implants Res 2005;16:650–6.
[70] Coelho PG, Bonfante EA, Pessoa RS, Marin C, Granato R, Giro G, et al. Characterization of five different implant surfaces and their effect on osseointegration: a study in dogs. J Periodontol 2011;82:742–50.
[71] Ronold HJ, Ellingsen JE. Effect of micro-roughness produced by TiO_2 blasting – tensile testing of bone attachment by using coin-shaped implants. Biomaterials 2002;23:4211–9.
[72] Klokkevold PR, Johnson P, Dadgostari S, Caputo A, Davies JE, Nishimura RD. Early endosseous integration enhanced by dual acid etching of titanium: a torque removal study in the rabbit. Clin Oral Implants Res 2001;12:350–7.
[73] Abrahamsson I, Zitzmann NU, Berglundh T, Wennerberg A, Lindhe J. Bone and soft tissue integration to titanium implants with different surface topography: an experimental study in the dog. Int J Oral Maxillofac Implants 2001;16:323–32.
[74] Cochran DL, Schenk RK, Lussi A, Higginbottom FL, Buser D. Bone response to unloaded and loaded titanium implants with a sandblasted and acid-etched surface: a histometric study in the canine mandible. J Biomed Mater Res 1998;40:1–11.
[75] Schupbach P, Glauser R, Rocci A, Martignoni M, Sennerby L, Lundgren A, et al. The human bone-oxidized titanium implant interface: a light microscopic, scanning electron microscopic, back-scatter scanning electron microscopic, and energy-dispersive X-ray study of clinically retrieved dental implants. Clin Implant Dent Relat Res 2005;7(Suppl. 1):S36–43.
[76] Burgos PM, Rasmusson L, Meirelles L, Sennerby L. Early bone tissue responses to turned and oxidized implants in the rabbit tibia. Clin Implant Dent Relat Res 2008;10: 181–90.
[77] Sawase T, Jimbo R, Wennerberg A, Suketa N, Tanaka Y, Atsuta M. A novel characteristic of porous titanium oxide implants. Clin Oral Implants Res 2007;18:680–5.
[78] Jimbo R, Tovar N, Yoo DY, Janal MN, Anchieta RB, Coelho PG. The effect of different surgical drilling procedures on full laser-etched microgrooves surface-treated implants: an experimental study in sheep. Clin Oral Implants Res 2014;25(9):1072–7.
[79] Cei S, Legitimo A, Barachini S, Consolini R, Sammartino G, Mattii L, et al. Effect of laser micromachining of titanium

on viability and responsiveness of osteoblast-like cells. Implant Dent 2011;20:285–91.
[80] Kang SH, Cho SA. Comparison of removal torques for laser-treated titanium implants with anodized implants. J Craniofac Surg 2011;22:1491–5.
[81] Wennerberg A, Albrektsson T, Lausmaa J. Torque and histomorphometric evaluation of c.p. titanium screws blasted with 25- and 75-microns-sized particles of Al_2O_3. J Biomed Mater Res 1996;30:251–60.
[82] Albrektsson T, Wennerberg A. Oral implant surfaces. Part 1 – review focusing on topographic and chemical properties of different surfaces and in vivo responses to them. Int J Prosthodont 2004;17:536–43.
[83] Wennerberg A, Albrektsson T. Effects of titanium surface topography on bone integration: a systematic review. Clin Oral Implants Res 2009;20(Suppl. 4):172–84.
[84] Wennerberg A, Albrektsson T. On implant surfaces: a review of current knowledge and opinions. Int J Oral Maxillofac Implants 2010;25:63–74.
[85] Mertens C, Steveling HG. Early and immediate loading of titanium implants with fluoride-modified surfaces: results of 5-year prospective study. Clin Oral Implants Res 2011;22:1354–60.
[86] Albrektsson T, Branemark PI, Hansson HA, Lindstrom J. Osseointegrated titanium implants, requirements for ensuring a long-lasting, direct bone-to-implant anchorage in man. Acta Orthop Scand 1981;52:155–70.
[87] Khang W, Feldman S, Hawley CE, Gunsolley J. A multi-center study comparing dual acid-etched and machined-surfaced implants in various bone qualities. J Periodontol 2001;72:1384–90.
[88] Pinholt EM. Branemark and ITI dental implants in the human bone-grafted maxilla: a comparative evaluation. Clin Oral Implants Res 2003;14:584–92.
[89] Buddula A, Assad DA, Salinas TJ, Garces YI, Volz JE, Weaver AL. Survival of turned and roughened dental implants in irradiated head and neck cancer patients: a retrospective analysis. J Prosthet Dent 2011;106:290–6.
[90] Mendonca G, Mendonca DB, Aragao FJ, Cooper LF. Advancing dental implant surface technology – from micron- to nanotopography. Biomaterials 2008;29: 3822–35.
[91] Webster TJ, Ahn ES. Nanostructured biomaterials for tissue engineering bone. Adv Biochem Eng Biotechnol 2007;103:275–308.
[92] Gittens RA, Olivares-Navarrete R, McLachlan T, Cai Y, Hyzy SL, Schneider JM, et al. Differential responses of osteoblast lineage cells to nanotopographically-modified, microroughened titanium–aluminum–vanadium alloy surfaces. Biomaterials 2012;33:8986–94.
[93] Hayashi M, Jimbo R, Lindh L, Sotres J, Sawase T, Mustafa K, et al. In vitro characterization and osteoblast responses to nanostructured photocatalytic TiO_2 coated surfaces. Acta Biomater 2012;8:2411–6.
[94] Tomsia AP, Lee JS, Wegst UG, Saiz E. Nanotechnology for dental implants. Int J Oral Maxillofac Implants 2013;28:e535–46.
[95] Fröjd V, Franke-Stenport V, Meirelles L, Wennerberg A. Increased bone contact to a calcium-incorporated oxidized commercially pure titanium implant: an in-vivo study in rabbits. Int J Oral Maxillofac Surg 2008;37:561–6.
[96] Leach R. Fundamental principles of engineering nanometrology. William Andrew; 2009.
[97] Suri S, Ruan G, Winter J, Schmidt C. Microparticles and nanoparticles. In: Ratner B, Hoffman A, Schoen F, Lemons J, editors. Biomaterials science: an introduction to materials in medicine. San Diego, CA: Academic Press; 2013. p. 360–88.
[98] Cahay M.Quantum confinement. VI. Nanostructured materials and devices: Proceedings of the international symposium. The Electrochemical Society; 2001.
[99] Elias CN, Meirelles L. Improving osseointegration of dental implants. Expert Rev Med Devices 2010;7:241–56.
[100] Fridman A. Organic and polymer plasma chemistry. In: Plasma chemistry. Cambridge: Cambridge University Press; 2008. p. 589–675.
[101] Owens DK, Wendt R. Estimation of the surface free energy of polymers. J Appl Polym Sci 1969;13:1741–50.
[102] Kaelble D. Dispersion-polar surface tension properties of organic solids. J Adhes 1970;2:66–81.
[103] Żenkiewicz M. Methods for the calculation of surface free energy of solids. J Achiev Mater Manuf Eng 2007;24:137–45.
[104] Janssen D, De Palma R, Verlaak S, Heremans P, Dehaen W. Static solvent contact angle measurements, surface free energy and wettability determination of various self-assembled monolayers on silicon dioxide. Thin Solid Films 2006;515:1433–40.
[105] Rupp F, Scheideler L, Eichler M, Geis-Gerstorfer J. Wetting behavior of dental implants. Int J Oral Maxillofac Implants 2011;26:1256–66.
[106] Gittens RA, McLachlan T, Olivares-Navarrete R, Cai Y, Berner S, Tannenbaum R, et al. The effects of combined micron-/submicron-scale surface roughness and nanoscale features on cell proliferation and differentiation. Biomaterials 2011;32:3395–403.
[107] Biggs MJ, Richards RG, Gadegaard N, McMurray RJ, Affrossman S, Wilkinson CD, et al. Interactions with nanoscale topography: adhesion quantification and signal transduction in cells of osteogenic and multipotent lineage. J Biomed Mater Res A 2009;91:195–208.
[108] Dalby MJ, McCloy D, Robertson M, Wilkinson CD, Oreffo RO. Osteoprogenitor response to defined topographies with nanoscale depths. Biomaterials 2006;27:1306–15.
[109] Palin E, Liu H, Webster TJ. Mimicking the nanofeatures of bone increases bone-forming cell adhesion and proliferation. Nanotechnology 2005;16:1828.
[110] Webster TJ, Siegel RW, Bizios R. Osteoblast adhesion on nanophase ceramics. Biomaterials 1999;20:1221–7.
[111] Webster TJ, Ejiofor JU. Increased osteoblast adhesion on nanophase metals: Ti, Ti6Al4V, and CoCrMo. Biomaterials 2004;25:4731–9.
[112] Webster TJ, Ergun C, Doremus RH, Siegel RW, Bizios R. Enhanced functions of osteoblasts on nanophase ceramics. Biomaterials 2000;21:1803–10.
[113] Meirelles L, Currie F, Jacobsson M, Albrektsson T, Wennerberg A. The effect of chemical and nanotopographical modifications on the early stages of osseointegration. Int J Oral Maxillofac Implants 2008;23:641–7.
[114] Wennerberg A, Galli S, Albrektsson T. Current knowledge about the hydrophilic and nanostructured SLActive surface. Clin Cosmet Investig Dent 2011;3:59.
[115] Granato R, Marin C, Suzuki M, Gil JN, Janal MN, Coelho PG. Biomechanical and histomorphometric evaluation of a thin ion beam bioceramic deposition on plateau root form implants: an experimental study in dogs. J Biomed Mater Res B Appl Biomater 2009;90:396–403.
[116] Albrektsson T. Hydroxyapatite-coated implants: a case against their use. J Oral Maxillofac Surg 1998;56:1312–20.
[117] Dohan Ehrenfest DM, Coelho PG, Kang BS, Sul YT, Albrektsson T. Classification of osseointegrated implant surfaces: materials, chemistry and topography. Trends Biotechnol 2010;28:198–206.
[118] Coelho PG, Granato R, Marin C, Bonfante EA, Janal MN, Suzuki M. Biomechanical and bone histomorphologic

evaluation of four surfaces on plateau root form implants: an experimental study in dogs. Oral Surg Oral Med Oral Pathol Oral Radiol Endod 2010;109:e39–45.
[119] Berglundh T, Abrahamsson I, Albouy JP, Lindhe J. Bone healing at implants with a fluoride-modified surface: an experimental study in dogs. Clin Oral Implants Res 2007;18:147–52.
[120] Jimbo R, Anchieta R, Baldassarri M, Granato R, Marin C, Teixeira HS, et al. Histomorphometry and bone mechanical property evolution around different implant systems at early healing stages: an experimental study in dogs. Implant Dent 2013;22:596–603.
[121] Bucci-Sabattini V, Cassinelli C, Coelho PG, Minnici A, Trani A, Dohan Ehrenfest DM. Effect of titanium implant surface nanoroughness and calcium phosphate low impregnation on bone cell activity in vitro. Oral Surg Oral Med Oral Pathol Oral Radiol Endod 2010;109:217–24.
[122] Moura CC, Machado JR, Silva MV, Rodrigues DB, Zanetta-Barbosa D, Jimbo R, et al. Evaluation of human polymorphonuclear behavior on textured titanium and calcium-phosphate coated surfaces. Biomed Mater 2013;8:035010.
[123] Moura CG, Souza MA, Kohal RJ, Dechichi P, Zanetta-Barbosa D, Jimbo R, et al. Evaluation of osteogenic cell culture and osteogenic/peripheral blood mononuclear human cell co-culture on modified titanium surfaces. Biomed Mater 2013;8:035002.
[124] Liu R, Lei T, Dusevich V, Yao X, Liu Y, Walker MP, et al. Surface characteristics and cell adhesion: a comparative study of four commercial dental implants. J Prosthodont 2013;22:641–51.
[125] Monjo M, Petzold C, Ramis JM, Lyngstadaas SP, Ellingsen JE. In vitro osteogenic properties of two dental implant surfaces. Int J Biomater 2012;2012, 181024.
[126] Guo J, Padilla RJ, Ambrose W, De Kok IJ, Cooper LF. The effect of hydrofluoric acid treatment of TiO2 grit blasted titanium implants on adherent osteoblast gene expression in vitro and in vivo. Biomaterials 2007;28:5418–25.
[127] Valencia S, Gretzer C, Cooper LF. Surface nanofeature effects on titanium-adherent human mesenchymal stem cells. Int J Oral Maxillofac Implants 2009;24:38–46.
[128] Coelho PG, Cardaropoli G, Suzuki M, Lemons JE. Early healing of nanothickness bioceramic coatings on dental implants. An experimental study in dogs. J Biomed Mater Res B Appl Biomater 2009;88:387–93.
[129] Coelho PG, Lemons JE. Physico/chemical characterization and in vivo evaluation of nanothickness bioceramic depositions on alumina-blasted/acid-etched Ti–6Al–4V implant surfaces. J Biomed Mater Res A 2009;90:351–61.
[130] Coelho PG, Suzuki M. Evaluation of an IBAD thin-film process as an alternative method for surface incorporation of bioceramics on dental implants: a study in dogs. J Appl Oral Sci 2005;13:87–92.
[131] Granato R, Marin C, Gil JN, Chuang SK, Dodson TB, Suzuki M, et al. Thin bioactive ceramic-coated alumina-blasted/acid-etched implant surface enhances biomechanical fixation of implants: an experimental study in dogs. Clin Implant Dent Relat Res 2011;13:87–94.
[132] Suzuki M, Calasans-Maia MD, Marin C, Granato R, Gil JN, Granjeiro JM, et al. Effect of surface modifications on early bone healing around plateau root form implants: an experimental study in rabbits. J Oral Maxillofac Surg 2010;68:1631–8.
[133] Suzuki M, Guimaraes MV, Marin C, Granato R, Gil JN, Coelho PG. Histomorphometric evaluation of alumina-blasted/acid-etched and thin ion beam-deposited bioceramic surfaces: an experimental study in dogs. J Oral Maxillofac Surg 2009;67:602–7.
[134] Quaranta A, Iezzi G, Scarano A, Coelho PG, Vozza I, Marincola M, et al. A histomorphometric study of nanothickness and plasma-sprayed calcium-phosphorous-coated implant surfaces in rabbit bone. J Periodontol 2010;81:556–61.
[135] Mendes VC, Moineddin R, Davies JE. The effect of discrete calcium phosphate nanocrystals on bone-bonding to titanium surfaces. Biomaterials 2007;28:4748–55.
[136] Mendes VC, Moineddin R, Davies JE. Discrete calcium phosphate nanocrystalline deposition enhances osteoconduction on titanium-based implant surfaces. J Biomed Mater Res A 2009;90:577–85.
[137] Lin A, Wang CJ, Kelly J, Gubbi P, Nishimura I. The role of titanium implant surface modification with hydroxyapatite nanoparticles in progressive early bone-implant fixation in vivo. Int J Oral Maxillofac Implants 2009;24:808–16.
[138] Calvo-Guirado JL, Satorres-Nieto M, Aguilar-Salvatierra A, Delgado-Ruiz RA, Mate-Sanchez de Val JE, Gargallo-Albiol J, et al. Influence of surface treatment on osseointegration of dental implants: histological, histomorphometric and radiological analysis in vivo. Clin Oral Investig 2014, http://dx.doi.org/10.1007/s00784-014-1241-2. Apr 16. [Epub ahead of print].
[139] Calvo-Guirado JL, Satorres M, Negri B, Ramirez-Fernandez P, Mate-Sanchez JE, Delgado-Ruiz R, et al. Biomechanical and histological evaluation of four different titanium implant surface modifications: an experimental study in the rabbit tibia. Clin Oral Investig 2014;18:1495–505.
[140] Abrahamsson I, Linder E, Larsson L, Berglundh T. Deposition of nanometer scaled calcium-phosphate crystals to implants with a dual acid-etched surface does not improve early tissue integration. Clin Oral Implants Res 2013;24:57–62.
[141] Vignoletti F, Johansson C, Albrektsson T, De Sanctis M, San Roman F, Sanz M. Early healing of implants placed into fresh extraction sockets: an experimental study in the beagle dog. De novo bone formation. J Clin Periodontol 2009;36:265–77.
[142] Bonfante EA, Janal MN, Granato R, Marin C, Suzuki M, Tovar N, et al. Buccal and lingual bone level alterations after immediate implantation of four implant surfaces: a study in dogs. Clin Oral Implants Res 2013;24:1375–80.
[143] Choi JY, Lee HJ, Jang JU, Yeo IS. Comparison between bioactive fluoride modified and bioinert anodically oxidized implant surfaces in early bone response using rabbit tibia model. Implant Dent 2012;21:124–8.
[144] Heitz-Mayfield LJ, Darby I, Heitz F, Chen S. Preservation of crestal bone by implant design. A comparative study in minipigs. Clin Oral Implants Res 2013;24:243–9.
[145] Alharbi HM, Babay N, Alzoman H, Basudan S, Anil S, Jansen JA. Bone morphology changes around two types of bone-level implants installed in fresh extraction sockets – a histomorphometric study in Beagle dogs. Clin Oral Implants Res 2014, http://dx.doi.org/10.1111/clr.12388. Apr 2. [Epub ahead of print].
[146] de Sanctis M, Vignoletti F, Discepoli N, Munoz F, Sanz M. Immediate implants at fresh extraction sockets: an experimental study in the beagle dog comparing four different implant systems. Soft tissue findings. J Clin Periodontol 2010;37:769–76.
[147] Araujo MG, Sukekava F, Wennstrom JL, Lindhe J. Tissue modeling following implant placement in fresh extraction sockets. Clin Oral Implants Res 2006;17:615–24.
[148] Araujo MG, Wennstrom JL, Lindhe J. Modeling of the buccal and lingual bone walls of fresh extraction sites following

implant installation. Clin Oral Implants Res 2006;17:606–14.
[149] Marin C, Granato R, Suzuki M, Gil JN, Piattelli A, Coelho PG. Removal torque and histomorphometric evaluation of bioceramic grit-blasted/acid-etched and dual acid-etched implant surfaces: an experimental study in dogs. J Periodontol 2008;79:1929–42.
[150] Marin C, Granato R, Bonfante EA, Suzuki M, Janal MN, Coelho PG. Evaluation of a nanometer roughness scale resorbable media-processed surface: a study in dogs. Clin Oral Implants Res 2012;23:119–24.
[151] Coelho PG, Zavanelli RA, Salles MB, Yeniyol S, Tovar N, Jimbo R. Enhanced bone bonding to nanotextured implant surfaces. Biomechanical tensile testing in the rat femur; 2014 (Submitted for publication).
[152] Coelho PG, Granato R, Marin C, Jimbo R, Lin S, Witek L, et al. Effect of Si addition on Ca- and P-impregnated implant surfaces with nanometer-scale roughness: an experimental study in dogs. Clin Oral Implants Res 2012;23:373–8.
[153] Coelho PG, Takayama T, Yoo D, Jimbo R, Karunagaran S, Tovar N, et al. Nanometer-scale features on micrometer-scale surface texturing: a bone histological, gene expression, and nanomechanical study. Bone 2014;65C:25–32.
[154] Coelho PG, Marin C, Granato R, Bonfante EA, Lima CP, Suzuki M. Surface treatment at the cervical region and its effect on bone maintenance after immediate implantation: an experimental study in dogs. Oral Surg Oral Med Oral Pathol Oral Radiol Endod 2010;110:182–7.
[155] Coelho PG, Granato R, Marin C, Bonfante EA, Freire JN, Janal MN, et al. Biomechanical evaluation of endosseous implants at early implantation times: a study in dogs. J Oral Maxillofac Surg 2010;68:1667–75.
[156] Ostman PO, Wennerberg A, Ekestubbe A, Albrektsson T. Immediate occlusal loading of NanoTite tapered implants: a prospective 1-year clinical and radiographic study. Clin Implant Dent Relat Res 2013;15:809–18.
[157] Ostman PO, Wennerberg A, Albrektsson T. Immediate occlusal loading of NanoTite PREVAIL implants: a prospective 1-year clinical and radiographic study. Clin Implant Dent Relat Res 2010;12:39–47.
[158] Cecchinato D, Lops D, Salvi GE, Sanz M. A prospective, randomized, controlled study using OsseoSpeed implants placed in maxillary fresh extraction socket: soft tissues response. Clin Oral Implants Res 2013, http://dx.doi.org/10.1111/clr.12295. Dec 2. [Epub ahead of print].
[159] Collaert B, Wijnen L, De Bruyn H. A 2-year prospective study on immediate loading with fluoride-modified implants in the edentulous mandible. Clin Oral Implants Res 2011;22:1111–6.
[160] De Bruyn H, Raes F, Cooper LF, Reside G, Garriga JS, Tarrida LG, et al. Three-years clinical outcome of immediate provisionalization of single Osseospeed() implants in extraction sockets and healed ridges. Clin Oral Implants Res 2013;24:217–23.
[161] Mertens C, Steveling HG, Seeberger R, Hoffmann J, Freier K. Reconstruction of severely atrophied alveolar ridges with calvarial onlay bone grafts and dental implants. Clin Implant Dent Relat Res 2013;15:673–83.
[162] Noelken R, Neffe BA, Kunkel M, Wagner W. Maintenance of marginal bone support and soft tissue esthetics at immediately provisionalized OsseoSpeed implants placed into extraction sites: 2-year results. Clin Oral Implants Res 2014;25:214–20.
[163] Raes F, Cosyn J, De Bruyn H. Clinical, aesthetic, and patient-related outcome of immediately loaded single implants in the anterior maxilla: a prospective study in extraction sockets, healed ridges, and grafted sites. Clin Implant Dent Relat Res 2013;15:819–35.
[164] Jimbo R, Coelho PG, Bryington M, Baldassarri M, Tovar N, Currie F, et al. Nano hydroxyapatite-coated implants improve bone nanomechanical properties. J Dent Res 2012;91:1172–7.
[165] Luxresearch. Sizing nanotechnology's value chain; 2004. https://portal.luxresearchinc.com/research/document_excerpt/2650
[166] Papaspyridakos P, Chen CJ, Singh M, Weber HP, Gallucci GO. Success criteria in implant dentistry: a systematic review. J Dent Res 2012;91:242–8.
[167] Manoharan M. Research on the frontiers of materials science: the impact of nanotechnology on new material development. Technol Soc 2008;30:401–4.